nature medicine

Oncogenic *PIK3CA*-driven mammary tumors frequently recur via PI3K pathway–dependent and PI3K pathway–independent mechanisms

Pixu Liu[1,2,11], Hailing Cheng[1–3,11], Stephanie Santiago[1,2], Maria Raeder[1,4], Fan Zhang[5], Adam Isabella[1], Janet Yang[1], Derek J Semaan[1], Changzhong Chen[6], Edward A Fox[6–8], Nathanael S Gray[1,2], John Monahan[9], Robert Schlegel[9], Rameen Beroukhim[1,7,8,10], Gordon B Mills[5] & Jean J Zhao[1–3]

PIK3CA **gain-of-function mutations are a common oncogenic event in human malignancy[1–4], making phosphatidylinositol 3-kinase (PI3K) a target for cancer therapy. Despite the promise of targeted therapy, resistance often develops, leading to treatment failure. To elucidate mechanisms of resistance to PI3K-targeted therapy, we constructed a mouse model of breast cancer conditionally expressing human *PIK3CA*^{H1047R}. Notably, most *PIK3CA*^{H1047R}-driven mammary tumors recurred after *PIK3CA*^{H1047R} inactivation. Genomic analyses of recurrent tumors revealed multiple lesions, including focal amplification of *Met* or *Myc* (also known as *c-Met* and *c-Myc*, respectively). Whereas *Met* amplification led to tumor survival dependent on activation of endogenous PI3K, tumors with *Myc* amplification became independent of the PI3K pathway. Functional analyses showed that *Myc* contributed to oncogene independence and resistance to PI3K inhibition. Notably, *PIK3CA* mutations and c-MYC elevation co-occur in a substantial fraction of human breast tumors. Together, these data suggest that c-MYC elevation represents a potential mechanism by which tumors develop resistance to current PI3K-targeted therapies.**

More than 25% of breast cancers harbor somatic mutations in the *PIK3CA*-encoded p110α catalytic subunit of PI3K[1–4]. These mutations usually occur in the helical region (E545K and E542K) or the kinase domain (H1047R) of p110α; H1047R is the most common mutation (>50% of cases). Several experimental models have demonstrated that these tumor-associated *PIK3CA* mutations lead to constitutive p110α activation and oncogenic transformation[5–9], making the *PIK3CA* oncogene a target for cancer therapy.

To study the effects of mutational activation of PI3K on breast tumorigenesis *in vivo* and to identify potential mechanisms of resistance to PI3K inhibition, we generated a transgenic mouse line expressing human *PIK3CA*^{H1047R} in which transgene expression is under the control of a tetracycline-inducible promoter (TetO). *PIK3CA*^{H1047R} expression is coupled with a luciferase reporter allowing transgene expression to be followed *in vivo* (**Fig. 1a**). To drive mammary-specific expression of *PIK3CA*^{H1047R}, we crossed two TetO-*PIK3CA*^{H1047R} founders (HR-2239 and HR-2251) to a previously described MMTV-rtTA (MTB) line[10]. The resulting bitransgenic MTB/TetO-*PIK3CA*^{H1047R} mice were designated iPIK3CA^{H1047R}. Quantitative RT-PCR analyses of mammary tissues isolated from bitransgenic females showed that doxycycline treatment led to a substantial increase in *PIK3CA*^{H1047R} expression and luciferase reporter activity, whereas endogenous mouse *Pik3ca* expression remained unaffected (**Supplementary Fig. 1a**,**b**). As mice derived from both iPIK3CA^{H1047R} founder lines showed comparable mammary gland-specific and doxycycline-dependent transgene expression, we used the MTB/HR-2239 line for all subsequent experiments.

To determine whether expression of *PIK3CA*^{H1047R} can initiate transformation of mammary epithelium, we analyzed mammary glands isolated from iPIK3CA^{H1047R} females treated with doxycycline for 4 weeks. Histological examination showed increased mammary ductal side-branching and enlarged focal nodular structures filled with hyperproliferative cells characteristic of early neoplastic lesions (**Supplementary Fig. 2a**,**b**). Immunohistochemical analyses showed strong phospho-AKT (p-AKT) signals in proliferating epithelial cells in the mammary glands of doxycycline-treated mice (**Supplementary Fig. 2c**), indicating activation of PI3K signaling in response to the induction of *PIK3CA*^{H1047R}. Consistent with the phenotype noted above, chronic doxycycline induction of the *PIK3CA*^{H1047R} transgene in bitransgenic mice led to the development of mammary tumors with 95% penetrance and a mean latency of 7 months

[1]Department of Cancer Biology, Dana-Farber Cancer Institute, Boston, Massachusetts, USA. [2]Department of Biological Chemistry and Molecular Pharmacology, Harvard Medical School, Boston, Massachusetts, USA. [3]Department of Surgery, Brigham and Women's Hospital, Boston, Massachusetts, USA. [4]Department of Obstetrics and Gynecology, Haukeland University Hospital and Department of Clinical Medicine, University of Bergen, Bergen, Norway. [5]Department of Systems Biology, University of Texas M.D. Anderson Cancer Center, Houston, Texas, USA. [6]Microarray Core, Dana-Farber Cancer Institute, Boston, Massachusetts, USA. [7]Department of Medical Oncology, Dana-Farber Cancer Institute, Boston, Massachusetts, USA. [8]Department of Medicine, Harvard Medical School, Boston, Massachusetts, USA. [9]Novartis Institutes for Biomedical Research, Cambridge, Massachusetts, USA. [10]Broad Institute, Cambridge, Massachusetts, USA. [11]These authors contributed equally to this work. Correspondence should be addressed to J.J.Z. (jean_zhao@dfci.harvard.edu).

Received 10 December 2010; accepted 18 May 2011; published online 7 August 2011; doi:10.1038/nm.2402

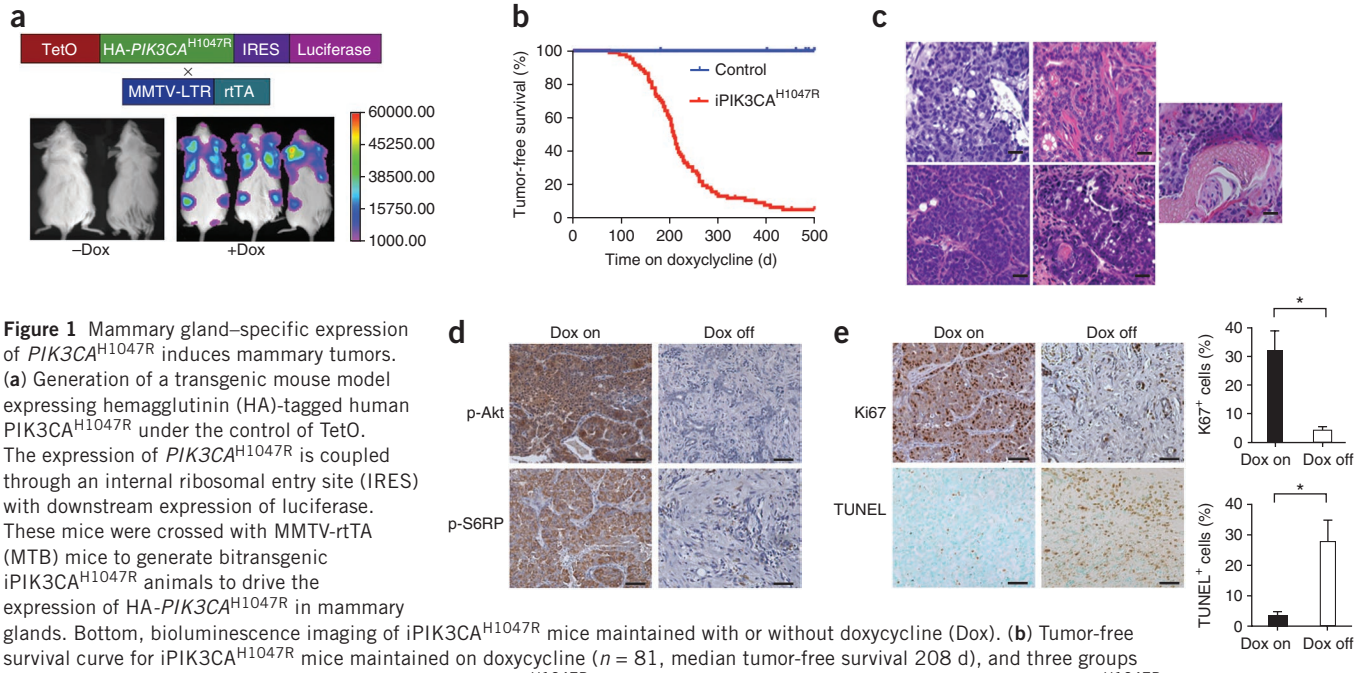

Figure 1 Mammary gland–specific expression of *PIK3CA*^{H1047R} induces mammary tumors. (**a**) Generation of a transgenic mouse model expressing hemagglutinin (HA)-tagged human PIK3CA^{H1047R} under the control of TetO. The expression of *PIK3CA*^{H1047R} is coupled through an internal ribosomal entry site (IRES) with downstream expression of luciferase. These mice were crossed with MMTV-rtTA (MTB) mice to generate bitransgenic iPIK3CA^{H1047R} animals to drive the expression of HA-*PIK3CA*^{H1047R} in mammary glands. Bottom, bioluminescence imaging of iPIK3CA^{H1047R} mice maintained with or without doxycycline (Dox). (**b**) Tumor-free survival curve for iPIK3CA^{H1047R} mice maintained on doxycycline ($n = 81$, median tumor-free survival 208 d), and three groups of control mice (blue line): MTB ($n = 12$) and TetO-*PIK3CA*^{H1047R} ($n = 10$) mice maintained with doxycycline, and iPIK3CA^{H1047R} ($n = 14$) mice maintained without doxycycline. (**c**) Representative H&E-stained sections of primary mammary tumors from iPIK3CA^{H1047R} mice subjected to chronic doxycycline treatment. Scale bars, 25 μm. (**d**) Representative images of immunohistochemistry for p-AKT (Ser473) and p-S6RP (Ser235 and Ser236) carried out on tumors isolated from iPIK3CA^{H1047R} mice maintained on doxycycline (Dox on) or 6 d after doxycycline withdrawal (Dox off). Scale bars, 50 μm. (**e**) Representative images of immunohistochemistry for Ki67 or TUNEL carried out on tumors isolated from iPIK3CA^{H1047R} mice maintained on doxycycline (Dox on) or 3 d after doxycycline withdrawal (Dox off). Scale bars, 50 μm. Data are means ± s.e.m. ($n = 6$). *$P < 0.005$ (Student's *t* test).

(**Fig. 1b**). These primary tumors had heterogeneous pathological phenotypes, including adenocarcinomas and adenosquamous carcinomas (**Fig. 1c** and **Supplementary Table 1**). In contrast, we observed no tumors in any of the control groups over the same time period (**Fig. 1b**). Thus, sustained induction of oncogenic *PIK3CA* expression leads to mammary tumor formation.

To examine whether established tumors required continued *PIK3CA*^{H1047R} expression to maintain their malignant state, we withdrew doxycycline from a cohort of tumor-bearing mice. All tumors regressed during the first week after doxycycline removal. We confirmed the suppression of *PIK3CA*^{H1047R} expression after doxycycline withdrawal by RT-PCR in primary tumors (**Supplementary Fig. 3**). Immunohistochemical analyses showed markedly lower abundance of both p-Akt and phospho-S6 ribosomal protein (p-S6RP) in tumors from which doxycycline was withdrawn as compared with those maintained on doxycycline (**Fig. 1d**). Moreover, although we detected a robust Ki67 signal in tumors maintained on doxycycline, there were significantly fewer proliferating cells after doxycycline withdrawal (**Fig. 1e**). Conversely, whereas we detected only a few apoptotic cells in tumors on doxycycline, we observed substantially more TUNEL-positive cells in tumors after doxycycline removal (**Fig. 1e**). These data indicate that reduced cellular

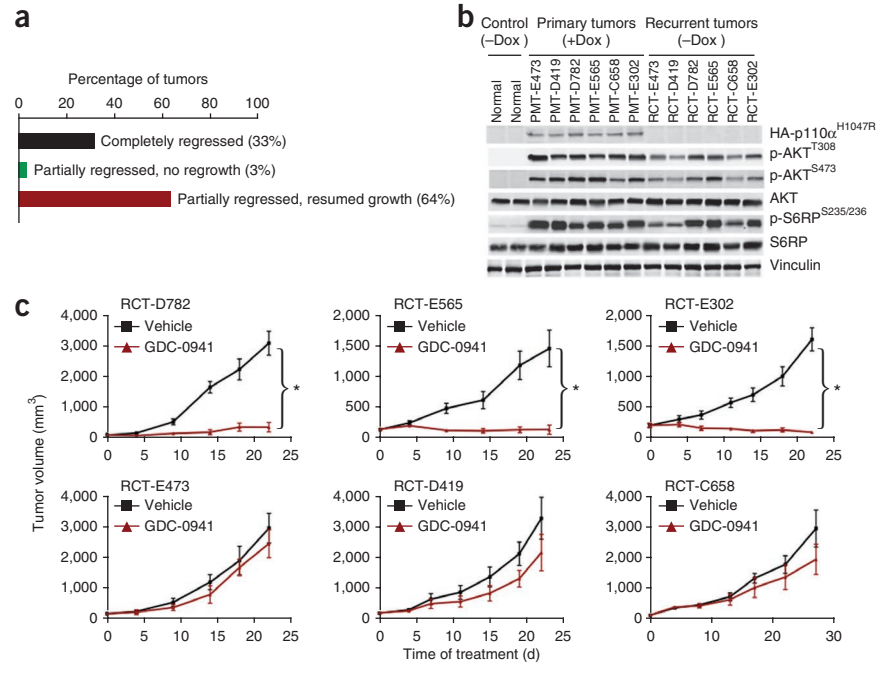

Figure 2 Tumor responses to doxycycline withdrawal. (**a**) Response of primary tumors (135 primary tumors derived from 107 tumor-bearing bitransgenic mice; 81 mice carried one tumor, 21 mice bore two tumors and 4 mice had three tumors) to doxycycline withdrawal. (**b**) Western blot analyses of HA-p110α^{H1047R}, p-Akt and p-S6RP in six recurrent tumors (RCT) without doxycycline and their matched primary tumors (PMT) maintained on doxycycline. Mammary gland tissues from uninduced iPIK3CA^{H1047R} mice were controls. (**c**) Responses of recurrent tumor transplants to GDC-0941 or vehicle treatment. Data are means ± s.e.m. ($n = 6$). *$P < 0.001$ (Student's *t* test).

proliferation and increased apoptosis are responsible for the initial phase of tumor regression after downregulation of oncogenic *PIK3CA*.

To determine whether the continued inactivation of oncogenic p110α^{H1047R} led to sustained regression of mammary carcinomas initiated by the expression of *PIK3CA*^{H1047R}, we followed a large cohort of tumors after doxycycline withdrawal for up to 6 months. We found that one-third of tumors (45 of 135, 33%) rapidly and completely regressed to a nonpalpable state within 1–2 months after doxycycline withdrawal with no regrowth (**Fig. 2a** and **Supplementary Fig. 4a**), indicating that these tumors remained dependent on p110α^{H1047R} for their maintenance. Although a small fraction of tumors (4 of 135, 3%) regressed partially and did not resume growth after doxycycline removal, about two-thirds of tumors (86 of 135, 64%) partially regressed but then resumed growth without doxycycline (**Fig. 2a** and **Supplementary Fig. 4b**). We confirmed that all recurrent tumors showed sustained downregulation of the *PIK3CA*^{H1047R} transgene and its protein product (**Fig. 2b**). Thus, *PIK3CA*^{H1047R}-initiated mammary tumors frequently did not regress completely upon *PIK3CA*^{H1047R} inactivation and recurred in a *PIK3CA*^{H1047R}-independent manner.

We next examined whether the PI3K pathway remained active in recurrent tumors, thus compensating for the loss of *PIK3CA*^{H1047R} expression. Western blot analyses of six paired primary and recurrent tumors showed that, although the phosphorylation levels of both AKT and S6RP were robust in all six primary tumors maintained on doxycycline, these signals were maintained in three recurrent tumors but were substantially lower in the other three (**Fig. 2b**). We then transplanted these six recurrent tumors into the mammary fat pads of athymic mice, and treated the tumor-bearing recipients with GDC-0941, a pan-Class I PI3K inhibitor currently in clinical trials[11,12]. Three recurrent tumors (RCT-D782, RCT-E565 and RCT-E302), all of which retained high abundance of both p-AKT and p-S6RP, were sensitive to GDC-0941 treatment (**Fig. 2c**). In contrast, the three recurrent tumors (RCT-E473, RCT-D419 and RCT-C658), which showed lower p-AKT and p-S6RP abundance, were resistant to GDC-0941 (**Fig. 2c**). These data suggest that some recurrent tumors escaped addiction to the oncogenic PIK3CA but remained dependent on the PI3K pathway, whereas others acquired the ability to grow independently of both the *PIK3CA* oncogene and the PI3K pathway.

To search for genomic aberrations associated with this recurrence, we carried out mouse single nucleotide polymorphism (SNP) array analyses of six recurrent tumors. A GDC-0941-sensitive tumor, RCT-E565, had a narrow amplification region encompassing *Met* (**Fig. 3a**) and also harbored a single-copy loss of the tumor suppressor gene *Cdkn2a* (**Supplementary Fig. 5a**). Notably, two of three tumors that were resistant to GDC-0941 had a common amplification on chromosome 15 spanning 1.48 megabases (chromosome 15:61,271,320–62,750,432), which contains the coding sequence for a single gene, *Myc* (**Fig. 3b**

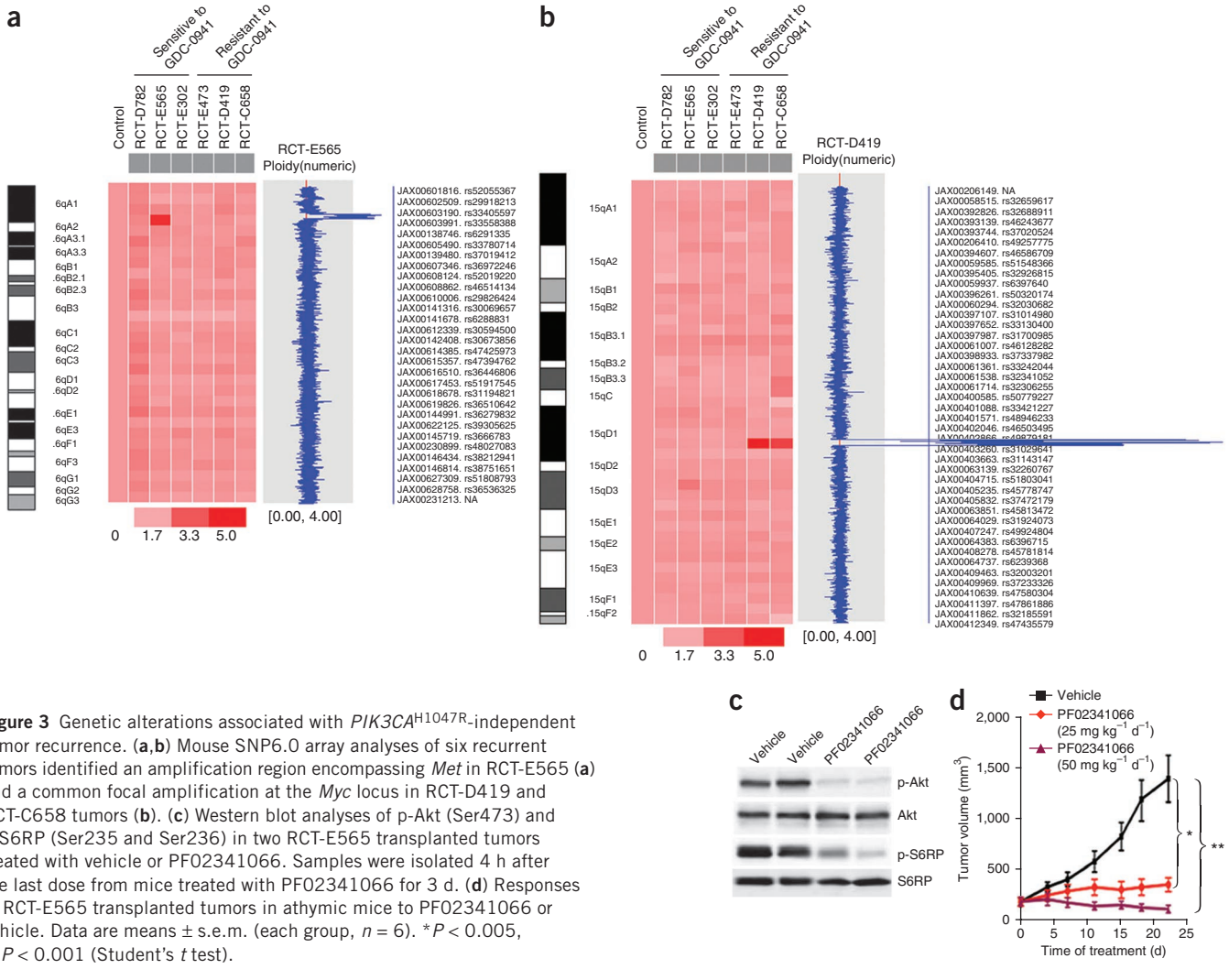

Figure 3 Genetic alterations associated with *PIK3CA*^{H1047R}-independent tumor recurrence. (**a**,**b**) Mouse SNP6.0 array analyses of six recurrent tumors identified an amplification region encompassing *Met* in RCT-E565 (**a**) and a common focal amplification at the *Myc* locus in RCT-D419 and RCT-C658 tumors (**b**). (**c**) Western blot analyses of p-Akt (Ser473) and p-S6RP (Ser235 and Ser236) in two RCT-E565 transplanted tumors treated with vehicle or PF02341066. Samples were isolated 4 h after the last dose from mice treated with PF02341066 for 3 d. (**d**) Responses of RCT-E565 transplanted tumors in athymic mice to PF02341066 or vehicle. Data are means ± s.e.m. (each group, $n = 6$). $^{*}P < 0.005$, $^{**}P < 0.001$ (Student's t test).

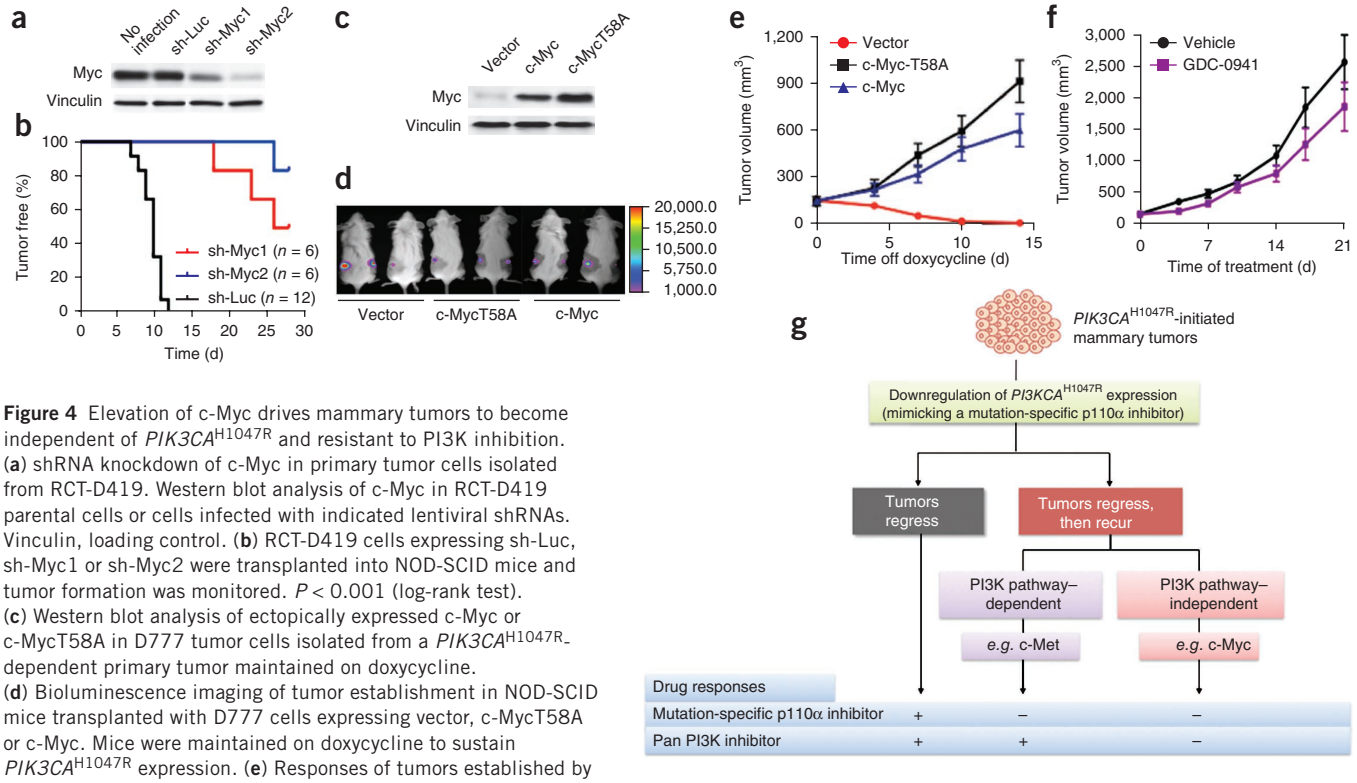

Figure 4 Elevation of c-Myc drives mammary tumors to become independent of *PIK3CA*^{H1047R} and resistant to PI3K inhibition. (**a**) shRNA knockdown of c-Myc in primary tumor cells isolated from RCT-D419. Western blot analysis of c-Myc in RCT-D419 parental cells or cells infected with indicated lentiviral shRNAs. Vinculin, loading control. (**b**) RCT-D419 cells expressing sh-Luc, sh-Myc1 or sh-Myc2 were transplanted into NOD-SCID mice and tumor formation was monitored. $P < 0.001$ (log-rank test). (**c**) Western blot analysis of ectopically expressed c-Myc or c-MycT58A in D777 tumor cells isolated from a *PIK3CA*^{H1047R}-dependent primary tumor maintained on doxycycline. (**d**) Bioluminescence imaging of tumor establishment in NOD-SCID mice transplanted with D777 cells expressing vector, c-MycT58A or c-Myc. Mice were maintained on doxycycline to sustain *PIK3CA*^{H1047R} expression. (**e**) Responses of tumors established by D777 cells expressing control vector, c-Myc or c-MycT58A to doxycycline withdrawal. Data are means ± s.e.m. ($n = 6$). (**f**) Mice bearing D777-MycT58A tumors were treated with either GDC-0941 or vehicle and tumor growth was monitored. Data are means ± s.e.m. ($n = 6$). (**g**) Schematic summarizing three outcomes of *PIK3CA*^{H1047R}-initiated tumors after inactivation of *PIK3CA*^{H1047R} expression.

and **Supplementary Fig. 6**). In addition to *Myc* amplification, RCT-C658 also carried an amplification encompassing the *Mdm2* oncogene (**Supplementary Fig. 5b**). Further analyses of c-Met, c-Myc and Mdm2 in a large collection of recurrent tumors showed that these oncogenes were upregulated in various fractions of recurrent tumors (**Supplementary Figs. 7–12** and **Supplementary Table 2**). These data demonstrate that several of the most common gain- or loss-of-function genetic events in human cancers were recapitulated in this mouse tumor model.

Because c-Met is a receptor tyrosine kinase that activates the PI3K pathway via ERBB3 and GAB1 (refs. 13,14), we tested whether *Met* amplification contributes to greater PI3K activity and tumor growth in the absence of *PIK3CA*^{H1047R} expression. We confirmed that the RCT-E565 tumor, but not its parental primary tumor PMT-E565, had elevated c-Met mRNA and protein expression (**Supplementary Fig. 13**). We then treated mice bearing RCT-E565 tumor transplants with PF02341066, a c-Met inhibitor currently in clinical development[15]. PF02341066 abrogated both p-Akt and p-S6RP signals as well as tumor growth (**Fig. 3c**,**d**). These results suggest that c-Met elevation is a mechanism underlying the growth of recurrent tumors that have escaped oncogenic *PIK3CA* addiction but remain dependent on the PI3K pathway.

Because two of three GDC-0941-insensitive recurrent tumors featured *Myc* amplification (**Fig. 3b**) and overexpression (**Supplementary Fig. 14**), and as c-Myc functions downstream of the PI3K pathway[16], we hypothesized that c-Myc elevation might contribute to the recurrence of tumors that were resistant to PI3K inhibition. Further analyses of c-Myc for DNA copy number and both mRNA and protein expression in a large cohort of recurrent tumors (**Supplementary Figs. 7–10**) showed that c-Myc elevation frequently occurs in recurrent tumors after sustained *PIK3CA*^{H1047R} inactivation. To test whether c-Myc elevation contributes to tumor recurrence in a PI3K pathway–independent manner, we examined the effects of *Myc* knockdown by shRNAs (sh-Myc1 and sh-Myc2) on the growth of recurrent tumors transplanted in the mammary fat pads of immunodeficient mice. Knockdown of *Myc* led to markedly lower tumor incidence and longer time to tumor onset (**Fig. 4a**,**b**). Conversely, enforced expression of c-Myc or c-MycT58A, a more stable version of c-Myc[17], rendered otherwise *PIK3CA*^{H1047R}-dependent tumors able to grow without doxycycline (**Fig. 4c–e**). Moreover, these c-Myc- or c-MycT58A-expressing tumors were resistant to GDC-0941 treatment (**Fig. 4f** and **Supplementary Fig. 15**). Together, these data suggest that c-Myc elevation renders tumors free of addiction to *PIK3CA*^{H1047R} and provides resistance to PI3K inhibition.

In our model, *PIK3CA*^{H1047R}-induced tumors have three potential outcomes in response to PI3K inhibition (**Fig. 4g**). For tumors that escape oncogene addiction and recur, c-Myc elevation represents a potential resistance mechanism with respect to current PI3K-targeted therapies in clinical trials. To explore whether *PIK3CA* mutations and c-MYC elevation coexist in human breast cancer, we analyzed several breast cancer data sets containing both PIK3CA mutation status and *MYC* copy number or expression data[18–21]. Among these cohorts, we found that substantial fractions of *PIK3CA* mutation–positive tumors have increased *MYC* copy numbers as well as mRNA and c-MYC protein levels[22,23] (**Supplementary Fig. 16** and **Supplementary Table 3**). Taken together, our findings suggest that aberrant elevation of c-MYC is a potential mechanism by which tumors develop resistance to PI3K inhibition, and thus combination therapies targeting both PI3K and c-MYC may be necessary to circumvent resistance to PI3K-targeted therapy.

METHODS

Methods and any associated references are available in the online version of the paper at http://www.nature.com/naturemedicine/.

Accession codes. SNP data are deposited in the Gene Expression Omnibus (GEO) with accession number GSE27691.

Note: Supplementary information is available on the Nature Medicine website.

ACKNOWLEDGMENTS

We thank T. Roberts, L. Cantley and W. Sellers for scientific discussions and suggestions. We thank L. Clayton and D. Silver for critical review of this manuscript. We thank R. Bronson for pathological analyses of tumor samples. We thank C. Li and E. Allgood for technical assistance. We thank L. Chodosh (University of Pennsylvania School of Medicine) for providing MMTV-rtTA mice. This work was supported by US National Institutes of Health grants CA134502 (J.J.Z.), CA148164-01 (J.J.Z. and N.S.G.) and K08CA122833 (R.B.), Stand Up To Cancer (J.J.Z. and G.B.M.), Dana Farber Harvard Cancer Center breast cancer SPORE grant P50 CA089393-08S1 (J.J.Z.), the US Department of Defense (BC051565 to J.J.Z.), the V Foundation (J.J.Z. and R.B.) and the Claudia Barr Program (J.J.Z.). In compliance with Harvard Medical School guidelines, we disclose that J.J.Z. and R.B. are consultants for Novartis Pharmaceuticals.

AUTHOR CONTRIBUTIONS

P.L., H.C. and J.J.Z. designed the experiments, interpreted the data and wrote the paper. P.L. and H.C. carried out most of the experiments. S.S., A.I. and D.J.S. assisted with biochemical analyses and mouse work. J.Y., C.C., E.A.F., J.M. and R.S. carried out genome-wide DNA copy number profiling. N.S.G. provided GDC-0941 inhibitor. M.R. and R.B. analyzed co-occurrence of PIK3CA mutation with c-MYC amplification and overexpression in human breast tumors. F.Z. and G.B.M. provided the reverse-phase protein array data on the co-occurrence of PIK3CA mutation with increased c-MYC expression in human breast tumors.

COMPETING FINANCIAL INTERESTS

The authors declare no competing financial interests.

Published online at http://www.nature.com/naturemedicine/.
Reprints and permissions information is available online at http://www.nature.com/reprints/index.html.

1. Samuels, Y. *et al.* High frequency of mutations of the PIK3CA gene in human cancers. *Science* **304**, 554 (2004).
2. Liu, P., Cheng, H., Roberts, T.M. & Zhao, J.J. Targeting the phosphoinositide 3-kinase pathway in cancer. *Nat. Rev. Drug Discov.* **8**, 627–644 (2009).
3. Vogt, P.K., Kang, S., Elsliger, M.A. & Gymnopoulos, M. Cancer-specific mutations in phosphatidylinositol 3-kinase. *Trends Biochem. Sci.* **32**, 342–349 (2007).
4. Yuan, T.L. & Cantley, L.C. PI3K pathway alterations in cancer: variations on a theme. *Oncogene* **27**, 5497–5510 (2008).
5. Zhao, J.J. *et al.* The oncogenic properties of mutant p110α and p110β phosphatidylinositol 3-kinases in human mammary epithelial cells. *Proc. Natl. Acad. Sci. USA* **102**, 18443–18448 (2005).
6. Kang, S., Bader, A.G. & Vogt, P.K. Phosphatidylinositol 3-kinase mutations identified in human cancer are oncogenic. *Proc. Natl. Acad. Sci. USA* **102**, 802–807 (2005).
7. Isakoff, S.J. *et al.* Breast cancer-associated PIK3CA mutations are oncogenic in mammary epithelial cells. *Cancer Res.* **65**, 10992–11000 (2005).
8. Samuels, Y. *et al.* Mutant PIK3CA promotes cell growth and invasion of human cancer cells. *Cancer Cell* **7**, 561–573 (2005).
9. Engelman, J.A. *et al.* Effective use of PI3K and MEK inhibitors to treat mutant Kras G12D and PIK3CA H1047R murine lung cancers. *Nat. Med.* **14**, 1351–1356 (2008).
10. Gunther, E.J. *et al.* A novel doxycycline-inducible system for the transgenic analysis of mammary gland biology. *FASEB J.* **16**, 283–292 (2002).
11. Raynaud, F.I. *et al.* Biological properties of potent inhibitors of class I phosphatidylinositide 3-kinases: from PI-103 through PI-540, PI-620 to the oral agent GDC-0941. *Mol. Cancer Ther.* **8**, 1725–1738 (2009).
12. O'Brien, C. *et al.* Predictive biomarkers of sensitivity to the phosphatidylinositol 3′ kinase inhibitor GDC-0941 in breast cancer preclinical models. *Clin. Cancer Res.* **16**, 3670–3683 (2010).
13. Engelman, J.A. *et al.* MET amplification leads to gefitinib resistance in lung cancer by activating ERBB3 signaling. *Science* **316**, 1039–1043 (2007).
14. Turke, A.B. *et al.* Preexistence and clonal selection of MET amplification in EGFR mutant NSCLC. *Cancer Cell* **17**, 77–88 (2010).
15. Zou, H.Y. *et al.* An orally available small-molecule inhibitor of c-Met, PF-2341066, exhibits cytoreductive antitumor efficacy through antiproliferative and antiangiogenic mechanisms. *Cancer Res.* **67**, 4408–4417 (2007).
16. Sears, R. *et al.* Multiple Ras-dependent phosphorylation pathways regulate Myc protein stability. *Genes Dev.* **14**, 2501–2514 (2000).
17. Yeh, E. *et al.* A signalling pathway controlling c-Myc degradation that impacts oncogenic transformation of human cells. *Nat. Cell Biol.* **6**, 308–318 (2004).
18. Cizkova, M. *et al.* Gene expression profiling reveals new aspects of PIK3CA mutation in ERα-positive breast cancer: major implication of the Wnt signaling pathway. *PLoS ONE* **5**, e15647 (2010).
19. Kan, Z. *et al.* Diverse somatic mutation patterns and pathway alterations in human cancers. *Nature* **466**, 869–873 (2010).
20. Haverty, P.M. *et al.* High-resolution genomic and expression analyses of copy number alterations in breast tumors. *Genes Chromosom. Cancer* **47**, 530–542 (2008).
21. Saal, L.H. *et al.* Poor prognosis in carcinoma is associated with a gene expression signature of aberrant PTEN tumor suppressor pathway activity. *Proc. Natl. Acad. Sci. USA* **104**, 7564–7569 (2007).
22. Stemke-Hale, K. *et al.* An integrative genomic and proteomic analysis of PIK3CA, PTEN and AKT mutations in breast cancer. *Cancer Res.* **68**, 6084–6091 (2008).
23. Tibes, R. *et al.* Reverse phase protein array: validation of a novel proteomic technology and utility for analysis of primary leukemia specimens and hematopoietic stem cells. *Mol. Cancer Ther.* **5**, 2512–2521 (2006).

ONLINE METHODS

Transgenic mice. We cloned human *PIK3CA*^{H1047R} into the BamHI site of pTRE2 (Clontech) and inserted an IRES-firefly luciferase sequence downstream of *PIK3CA*^{H1047R} to generate the TetO-*PIK3CA*^{H1047R}-IRES-luciferase plasmid. We linearized the plasmid and gel-purified the released fragment for injection into fertilized oocytes from superovulated FVB mice at the transgenic core facility at Brigham and Women's Hospital, Boston. We crossed TetO-*PIK3CA*^{H1047R} mice with MMTV-rtTA (MTB) mice (provided by L. Chodosh, University of Pennsylvania School of Medicine) to produce mice with inducible *PIK3CA*^{H1047R} transgene expression in mammary glands (iPIK3CA^{H1047R}). We administered iPIK3CA^{H1047R} mice with doxycycline in their drinking water (2 mg ml^{-1}). We carried out all mouse experiments in accordance with protocols approved by the Institutional Animal Care and Use Committees of Dana-Farber Cancer Institute and Harvard Medical School.

Bioluminescence imaging. We anesthetized mice with ketamine and xylazine and administered D-luciferin (Promega) intraperitoneally to monitor luciferase gene expression *in vivo*. We analyzed images with KODAK Molecular Imaging Software (version 4.5.0b6 SE).

Western blotting. We prepared lysates for mammary glands, mammary tumors or tumor cells in ice-cold RIPA buffer (Sigma-Aldrich) containing protease inhibitor cocktail (Roche). We cleared lysates by centrifugation before subjecting them to separation on SDS-PAGE and carried out western blot assays as described[5] with antibodies to p-AKT (Ser473 or Thr308), AKT, p-S6RP (Ser235 and Ser236), S6RP and c-Met (Cell Signaling Technology), c-Myc (Santa Cruz Biotechnology) and vinculin (Sigma-Aldrich). We used immunofluorescently labeled antibody to mouse IgG (Rockland Immunochemicals) and antibody to rabbit IgG (Molecular Probes) to visualize western blots on an Odyssey scanner (Li-Cor).

Histology and immunohistochemistry. We fixed tumors in formalin overnight before paraffin embedding. Paraffin blocks were sectioned and stained with H&E at the Dana-Farber/Harvard Cancer Center Rodent Histopathology Core. We carried out immunohistochemistry using the antibodies Ki67 (Vector), p-Akt (Ser473) (Invitrogen) and p-S6RP (Cell Signaling). We carried out TUNEL assays using the ApoTag Plus Peroxidase *in situ* TUNEL Apoptosis Kit (Millipore) according to the manufacturer's instructions.

Mouse SNP analyses. We isolated genomic DNA from mammary tissues or tumors using the Allprep DNA/RNA Kit (Qiagen). SNP array analyses with Mouse Diversity Genotyping Arrays (Affymetrix) were carried out at the Microarray Core at Dana-Farber Cancer Institute. The SNP data were analyzed using a SNP microarray copy number application[24] in the software suite dChip (http://biosun1.harvard.edu/complab/dchip/) to compare positions of copy difference between a normal tissue sample from the inbred strain of mouse used in this study and each of the tumor samples from the same inbred strain.

Tumor cell culture and viral transduction. We isolated tumors and dissociated them into single cells as described[25] with the exception that the cells were cultured in DMEM/F12 supplemented with 0.5% (vol/vol) FBS and 10 ng ml^{-1} epidermal growth factor and doxycycline (2 μg ml^{-1}). We produced retrovirus or lentivirus and infected cells according to the methods described[26,27]. Infected cells were selected in culture medium plus puromycin (0.5 μg ml^{-1}) for 2 d. Cells were passaged no more than twice before being used for injection or further analysis. The retroviral vectors used in this study were MSCV-PIG (Puro IRES GFP; used as control vector, Addgene plasmid 18751), MSCV-MYC-T58A (Addgene plasmid 20076) and MSCV-MYC (derived from MSCV-MYC-T58A by site-directed mutagenesis; Stratagene). The lentiviral shRNA constructs sh-Luc, shMyc-1 (TRCN 42513) and shMyc-2 (TRCN 42517) were obtained from the RNAi consortium (Broad Institute).

Tumor transplantation and *in vivo* treatment studies. For tumor grafting, we injected 2–5 × 10^5 tumor cells into the inguinal mammary glands of recipient mice (NcrNu or NOD-SCID females, 10–12 week old, Taconic). GDC-0941 was purchased from Sai Advantium Pharma and was reconstituted in 0.5% (wt/vol) methylcellulose (Sigma) and 0.2% (vol/vol) Tween 80 (Sigma) and administered by oral gavage (120 mg kg^{-1} d^{-1}). PF02341066 (Selleck Chemicals) was administered via oral gavage at doses of 25 or 50 mg kg^{-1} d^{-1} in water. Tumor volumes were measured twice a week with calipers and calculated using the following formula: tumor volume = (length × width^2)/2 (ref. 28).

Statistical analyses. We analyzed mammary tumor-free survival using Kaplan-Meier log-rank test. We analyzed quantitative results by two-tailed unpaired Student's *t* test. $P < 0.05$ was considered statistically significant.

Additional methods. Detailed methodology is described in the **Supplementary Methods**.

24. Zhao, X. *et al.* An integrated view of copy number and allelic alterations in the cancer genome using single nucleotide polymorphism arrays. *Cancer Res.* **64**, 3060–3071 (2004).
25. Moody, S.E. *et al.* Conditional activation of Neu in the mammary epithelium of transgenic mice results in reversible pulmonary metastasis. *Cancer Cell* **2**, 451–461 (2002).
26. Moffat, J. *et al.* A lentiviral RNAi library for human and mouse genes applied to an arrayed viral high-content screen. *Cell* **124**, 1283–1298 (2006).
27. Moody, S.E. *et al.* The transcriptional repressor Snail promotes mammary tumor recurrence. *Cancer Cell* **8**, 197–209 (2005).
28. Tomayko, M.M. & Reynolds, C.P. Determination of subcutaneous tumor size in athymic (nude) mice. *Cancer Chemother. Pharmacol.* **24**, 148–154 (1989).